

Design and Implementation of an Area-Efficient MEMS-Based IR Static Earth Sensor

Ahmed Salah, Ashraf Adel, Ahmed Ezeldin,
Ahmed Ali, Ahmed Hussein, and Serag E.-D. Habib

Abstract— This paper introduces a complete design of a static earth sensor, used for satellite attitude determination. Our design approach offers high area efficiency, high resolution (10 arc minutes), and modularity relative to previous designs. This sensor is made up of four separate identical chips; each chip represents a complete System on Chip (SoC) including the following main components: the sensor, the electronic read-out sub-circuit, the decision sub-circuit, and the serial interface to the On-Board Computer (OBC). Each chip has two staggered arrays of MEMS bulk-micromachined thermopiles, which sense the IR radiation incident on the chip and convert it into an electrical voltage. A complete design of the IR detector is introduced and its characteristics are estimated. A novel block diagram of one chip is presented including both analog and digital sub-circuits. A low offset amplifier (LOA), based on the Auto-zeroing technique, is used as a front-end to the analog part of the circuit. Finally, a complete layout of the SoC is given.

Index Terms— Auto-zeroing, MEMS, SoC, Static Earth Sensor, Thermopile.

I. INTRODUCTION

MEMS (Micro-Electro-Mechanical Systems) technology is the integration of mechanical elements, sensors, actuators, and electronics on a common silicon substrate. The main methods for MEMS Fabrication are bulk micromachining, surface micromachining, and LIGA [1] [2].

Satellite attitude determination is the process of computing the orientation of the satellite relative to some object of interest, such as the earth. Several types of sensors are used in the satellite attitude determination such as sun sensors, earth sensors, and star trackers [3].

The earth sensor is a thermal device, which determines the edges of the earth using the infrared (IR) radiation emitted from the earth. This keeps the sensor, and thus the platform, exactly oriented toward the earth. Several types of earth sensors are used for satellite attitude determination, such as the scanning earth sensors using two bolometers, the scanning earth sensors using single IR detector, the spinning earth sensors [4], and the static earth sensors.

The outline of this paper is as follows. In Section II, we describe the basic idea of the static earth sensor in addition to the advantages of our configuration. In Section III, we describe the complete pixel design including: the basic idea of thermopiles, the pixel characteristics, and the pixel layout.

Ahmed Salah, Ashraf Adel, Ahmed Ezeldin, Ahmed Ali, Ahmed Hussein are graduates from Cairo University, Faculty of Engineering, Electronics & Electrical Communications Dept. (e-mail: ahmed_salah@eng.cu.edu.eg).

Prof. Serag E.-D. Habib is a professor in the same Electronics & Electrical Communications Dept. (e-mail: seraged@ieec.org).

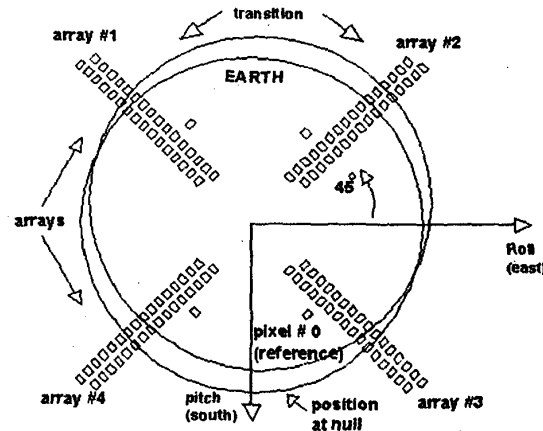


Fig. 1. Sensor Arrays Configuration

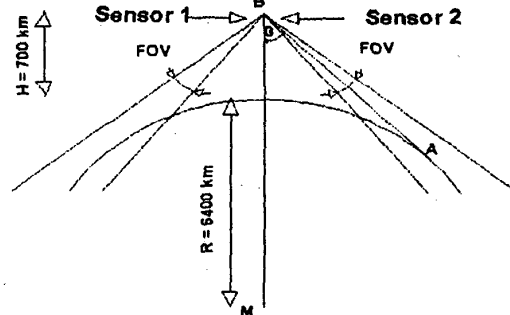


Fig. 2. Two Sensors Orientation

In Section IV, we describe the complete design of the chip, mainly the analog read-out sub-circuit and the digital decision sub-circuit. Finally, section V contains the conclusions.

II. STATIC EARTH SENSOR

The basic idea of the static earth sensor is to use four static arrays of IR detectors. They continuously look at the northwest, northeast, southwest, and southeast edges of Earth [5] [6]. The sensor detects any error in the position of the satellite, with respect to the earth, and sends it to the satellite's Attitude Control System (ACS), which corrects it.

In Fig. 1, each array consists of 32 pixels, which are arranged in two staggered arrays (each of 16 pixels) next to each other. In this configuration the four arrays of pixels (IR detectors) are on the same chip.

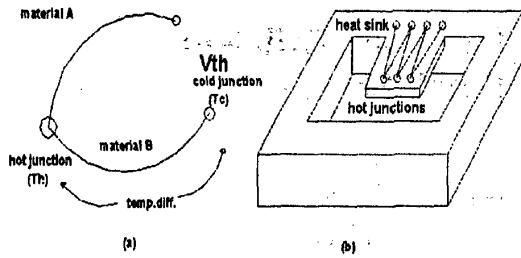


Fig. 3. Seebeck based devices: (a) thermocouple structure and (b) micromachined thermopile.

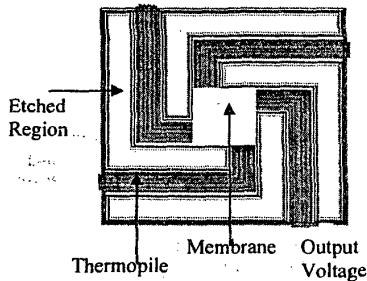


Fig. 4. Pixel Layout

The static earth sensor of Fig. 1 offers high reliability due to the absence of moving parts. However, the area Fill Factor is very low. In addition, the pixel resolution is low as the Field of View (FOV) needs to be greater than the angle subtended by the earth at the satellite position.

We introduce here another arrangement of the static earth sensor as depicted in Fig. 2. Four identical sensors, with higher Fill Factor, are used. Each sensor houses one arm and focuses the incident IR radiation of the earth on one of the four identical chips. This gives us high area efficiency due to avoiding the unused space inside the chip. Also, this smaller chip focuses the array of 32 pixels on a narrow FOV ($\approx 5^\circ$), which leads to higher resolution (≈ 10 arc minutes). So each chip represents a complete System on Chip (SoC) and includes the following main blocks: array of 32 pixels, analog read-out sub-circuit, digital decision sub-circuit, control sub-circuit, and the serial interface to the OBC.

Two pairs of the narrow FOV sensors are placed on two perpendicular axes. Each pair consists of two sensors pointing at an angle $\pm\theta$ off the Nadir direction, as shown in Fig. 2. Each sensor has a narrow FOV ($\approx 5^\circ$). The angle θ is given by:

$$\sin\theta = \frac{R}{R+H} \quad (1)$$

Where R is the earth radius and H is the satellite altitude above the earth. For $H = 700$ Km and $R=6400$ Km, then $\theta = 64.34^\circ$.

III. PIXEL DESIGN

Our earth sensor employs thermocouples, which are based on the Seebeck effect as shown in Fig. 3.a [1]. The thermocouple converts the incident IR radiation into an electrical voltage. The thermopile is the integration of thermocouples connected in series to increase the electrical voltage.

Pixel Size	234x234 μm^2
Membrane Size	72x72 μm^2
Arm Length	120 μm
Arm Width	27 μm
Arm and Membrane Thickness	4.7 μm
Average Metal (AL) Length	183.1 μm
Average PolySi Length	178.5 μm
Thermoelectric Voltage	0.287 mV
Responsivity	69.3 V/W
Thermal Time Constant	7.77msec
Al/PolySi Seebeck Coefficient	248 $\mu\text{V}/\text{K}$
Thermal Conductivity for Metal	237W/mk
Thermal Conductivity for PolySi	28W/mk
Arm Average Thermal Capacity	$2 \times 10^6 \text{ Jm}^{-3}\text{K}^{-1}$
Membrane Average Thermal Capacity	$2 \times 10^6 \text{ Jm}^{-3}\text{K}^{-1}$
Thermopile Resistance	89.328k Ω
Noise (Johnson) Voltage	0.12 μV
Noise (Johnson) Equivalent Power (NEP)	0.92 nW
Detectivity (D)	$2.47 \times 10^7 \text{ cmHz}^{1/2}/\text{W}$

Table 1. Pixel characteristics

The main reason of using MEMS is to thermally isolate the thermopiles from the substrate. This produces high temperature difference which leads to high electrical voltage difference, as shown in Fig. 3.b [1].

We need to calculate the amount of power received by the sensor from the earth. Let the area of the detector (sensor) be A_d , the area of the source (earth) be A_s , and the distance between source and detector be d . Then the power received within wavelength interval $d\lambda$ is given by:

$$P(\lambda) d\lambda = \frac{A_s A_d C_1}{\pi d^2 \lambda^5} \frac{d\lambda}{e^{hc/\lambda T} - 1} \quad (2)$$

Where $C_1 = 2\pi hc^2$ and $C_2 = \frac{hc}{k}$

Where c is the light speed in free space, h is the Plank constant, and k is the Boltzmann constant. Then, evaluating the integral over λ range from 14 – 16 μm , we get the total power by:

$$P(\text{incident}) = \int_{14}^{16} P(\lambda) \tau(\lambda) d\lambda = \begin{cases} 1.38 \times 10^{-3} A_d \text{ for } T = 300^\circ \text{K} \\ 0.61 \times 10^{-3} A_d \text{ for } T = 240^\circ \text{K} \end{cases} \quad (3)$$

Where $P(\text{incident})$ is in Watts and A_d is in cm^2 . $\tau(\lambda)$ is the atmosphere transmittance and approximately equal to 0.2 for λ in the range of 14 – 16 μm .

The optical front-end of the sensor selects the relevant IR λ range, and concentrates the incident radiation within this range on the pixels. We select the FOV of this optical sub-system to be equal to 5° . Consider an aperture area of 70 cm^2 with a Fill Factor = 0.1, then the power incident on one pixel is:

$$P(\text{one pixel}) = \frac{P(\text{incident})}{\text{Total number of pixels}}, \text{ Fill Factor} = 9.4404 \mu\text{W} \quad (4)$$

So the temperature difference between the hot and cold junctions due to N ($=20$) thermocouples is:

$$\Delta T = \frac{P(\text{one pixel}) \cdot \cos\theta}{N \cdot G_{\text{Thermocouple}}} = 0.0579 \text{ K} \quad (5)$$

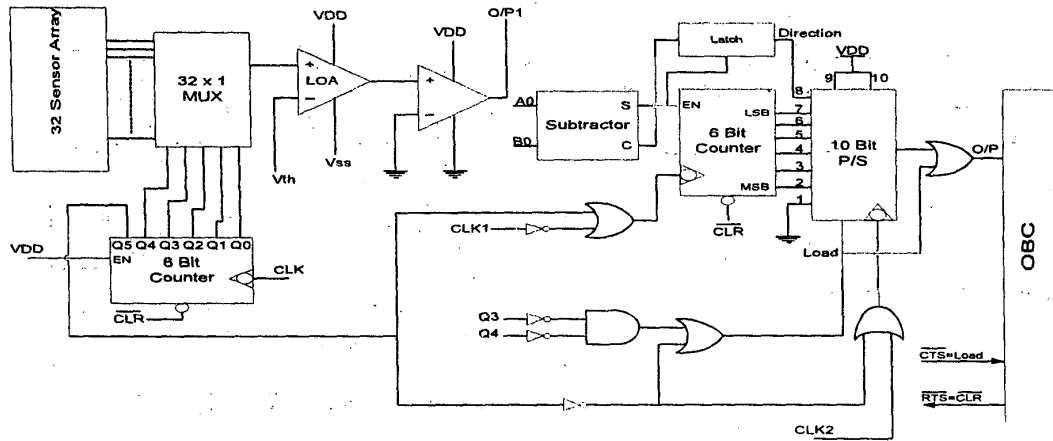


Fig. 5. Complete system block diagram

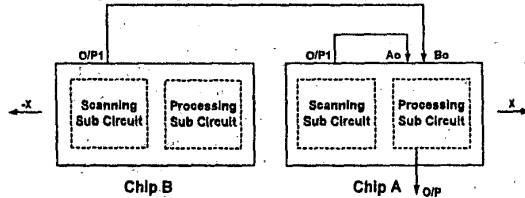


Fig. 6. Connection between two opposite chips

Where $G_{\text{Thermocouple}}$ is the total thermal conductance of one thermocouple, which is the summation of the thermal conductances of the Aluminum, the Poly Silicon and the substrate.

$$G_{\text{Thermocouple}} = G_{\text{Al}} + G_{\text{PolySi}} + G_{\text{Substrate}}$$

Using the Al/PolySi Seebeck coefficient (α), the output thermoelectric voltage difference is given by:

$$\Delta V(\text{pixel}) = N \cdot \alpha \cdot \Delta T = 0.287 \text{ mV} \quad (6)$$

The pixel characteristics are calculated, according to [7], as listed in Table 1. For the design of the pixel, we adopt the design rules of the $0.8\mu\text{m}$ CMOS CYE process from AMS [8].

Each pixel contains a thermopile made of 20 Al/Poly thermocouples, as shown in Fig. 4. The infrared radiation absorbed on the Si_3N_4 membrane will heat up the suspended micro-structure. The thermopiles placed on the support arms will sense the temperature gradient between the membrane and the substrate and produce an output voltage proportional to it [9].

IV. SYSTEM ON SHIP (SOC) DESIGN

The earth sensor detects any imbalance in the number of pixels illuminated on any two opposite arms. In the normal case, when comparing the two symmetric arrays of pixels, the total number of illuminated pixels (by the IR Radiation from the earth) in both arrays will be the same, thus the centre of those two arrays will be pointing to the earth centre. If there is a deviation by one pixel or more towards certain direction, then the total number of illuminated pixels in the two arrays will be different. Thus the satellite's Attitude Control System (ACS) has to correct this attitude error by rotating the satellite to return to the normal Nadir pointing attitude.

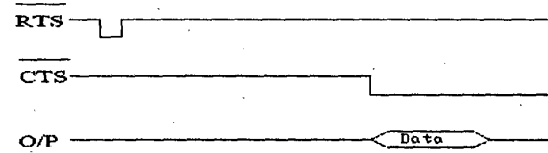


Fig. 7. Control Circuit Timing Diagram

The earth sensor sends the number of pixels to move and its direction to the OBC.

A reference pixel is used to determine if a pixel is illuminated or not. It always receives the maximum IR radiation from the earth, and produces only half of the maximum voltage produced by the normal array pixels, because it has half of the number of thermocouples.

Fig. 5 shows the complete system block diagram including: analog read-out sub-circuit, digital decision sub-circuit, and control sub-circuit. The system block diagram may be divided into two basic modules: scanning sub-circuit and processing sub-circuit.

The scanning sub-circuit is made up of: 1) Two staggered arrays of MEMS bulk-micromachined thermopiles and a reference pixel. 2) An analog multiplexer, which chooses the pixels' output voltage sequentially in synchronism with the pixels on the opposite arm. 3) A low offset amplifier (LOA), which amplifies the difference between the pixel voltage and the voltage of the reference pixel. 4) A comparator, which determines if the pixel is illuminated or not.

The processing sub-circuit is made up of: A) A subtractor that subtracts the two digital outputs coming from the two opposite arms of the sensor, to determine if they are the same or not. The connection of the two chips of the two opposite arms is as shown in Fig. 6. The processing sub-circuit is only active on chip A. B) A counter that counts the number of different pixels in the two opposite chips. C) A parallel-to-serial block diagram that prepares the serial interface to the OBC. D) A control sub-circuit that co-ordinates the operations of the blocks of the system, and consists of some logic gates.

The timing diagram shown in Fig. 7 shows the sequence of the signals done by the control sub-circuit. The OBC resets the RTS (Request to Send) signal and keeps it low for a certain time, then returns it high again.

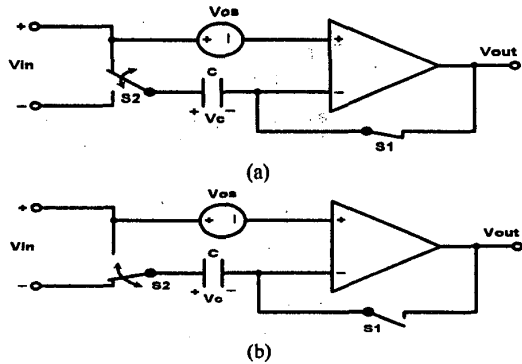


Fig. 8. Closed-loop amplifier offset cancellation principle: (a) offset sampling phase (AZ) and (b) amplification phase

This signal allows the chip to start scanning. After the chip finishes scanning of all the array pixels and determines the error pattern, the chip resets the CTS (Clear to Send) signal to send the error pattern through the output port.

One important component in the block diagram is the Low Offset Amplifier (LOA); its complete characteristics are shown in table 2. This amplifier accepts a pixel voltage of ($\sim 250 \mu\text{V}$), which is much smaller than the typical offset voltage of CMOS amplifiers. Auto-Zeroing Technique [10] is used in the design of the LOA, which reduces the applied (for testing) offset voltage from 5mv to only 0.1mv. As shown in Fig. 8, the OpAmp is represented by an ideal OpAmp, with zero offset voltage, connected to an offset voltage source. During the sampling phase, the amplifier is disconnected from the signal path and connected in a unity gain configuration as shown in Fig. 8 (a). The voltage V_c obtained across the storage capacitor C after the amplifier is almost equal to its offset voltage V_{os} ($V_c = V_{os}$). This voltage is stored across capacitor C since the input current of the amplifier is zero for a MOS input stage, and hence capacitor C behaves like a floating voltage source equal to V_{os} . After this sampling phase, an offset compensated stage is available for amplification and is connected again to the signal path. All other components are designed in a standard way.

All other required components have been designed and tested successfully. Also, their complete layout had been done according to AMS 0.8 μm CMOS CYE process with front-side bulk micromachining [8].

The main characteristics of the chip are shown in table 3. Also, Fig. 9 shows the complete chip layout, with labels pointing to the array of pixels, reference pixel, analog part, digital part and the pads.

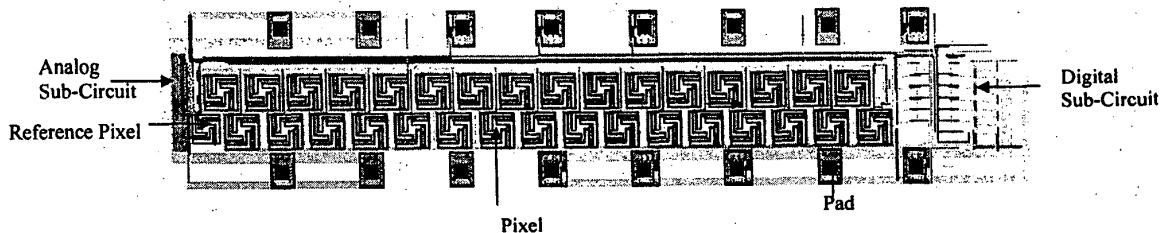


Fig. 9. Complete Chip Layout

DC Gain	68 db
Phase Margin	84°
3-DB Bandwidth	63 KHz
Unity Gain Frequency (f_u)	158 MHz
Input Noise	0.23 μV @ 2 KHz
Settling Time	45 nSec
Slew Rate (SR)	67 V/ μSec
Layout Area	148x80 μm^2
Total Power	1.158 mW
Number of Transistors	108

Table 2. Complete characteristics of OpAmp

Total Area	7mm ²
Total Power Dissipation	3 mW
V_{dd}	5v
V_{ss}	-5v

Table 3. Complete characteristics of one chip

V. CONCLUSION

We have introduced a new arrangement for a static earth sensor that achieves high area efficiency and high resolution. The sensor consists of 4 identical chips. Each chip contains: 1) The IR detector based on MEMS bulk-micromachined thermopile. 2) The analog read-out sub-circuit, the digital decision sub-circuit, the control sub-circuit, and the serial interface to the OBC. The complete design and layout of the single chip is introduced, and its characteristics are given.

REFERENCES

- [1] Renato P. Ribas, "Maskless Front-Side Bulk Micromachining Compatible to Standard GaAs IC Technology", TIMA-CMP.
- [2] www.allaboutmems.com
- [3] M.E. Koniger, "Sensors for Space Applications", IEEE Proceedings, pp. 3/68-3/738, May 1989.
- [4] Anderson J.D., Jump J.H., and O'Malley, J.W., "Autonomous Scan Management (ASM) for Earth Sensors", IEEE Aerospace Conference Proceedings, Vol. 2, pp. 445-451, 2000.
- [5] www.sodern.fr
- [6] Van Herwaarden, A.W., "Low-Cost Satellite Attitude Control Sensors Based on Integrated Infrared Detector Arrays", IEEE Transactions on Instrumentation and Measurement, Vol. 50, No. 6, pp. 1524-1529, Dec. 2001.
- [7] S. Sedky, "Uncooled Infrared Bolometers Based on Polycrystalline Silicon Germanium", Ph.D. thesis, Katholieke Universiteit Leuven, Belgium, Nov. 1998
- [8] "Design Rules For front side bulk micromachined structures Compatible with the 0.8 μm CMOS CYE process from AMS", Version 2, November 1999, Microsystem group, TIMA-CMP
- [9] B. Charlot, F. Parrain, S. Mir, and B. Courtois, "A Self-testable CMOS Thermopile-based Infrared Imager", TIMA Laboratory, private communication.
- [10] Christian C. Enz, Garbor C. Temes, "Circuit Techniques for Reducing the Effects of Op-Amp Imperfections: AutoZeroing, Correlated Double Sampling and Chopper Stabilization.", IEEE Proceedings, Vol. 84, No. 11, Nov. 1996.